MELT STABILIZATION of PbSnTe in a MAGNETIC FIELD

Archibald L. Fripp[a], William J. Debnam[b], William Rosch[c], Arnon Chait[d], Minwu Yao[e], and Frank R. Szofran[f]

541-27

1. INTRODUCTION

Both the experimental observation [1] and numerical simulation [2] indicate that the Bridgman growth of PbSnTe under the microgravity environment in space is still greatly influenced by buoyancy-induced convection. The application of a magnetic field during the semiconductor growth can dampen the convective flow in the metal-like melt [3-5]. However, for Bridgman growth of PbSnTe on earth (with either vertical or horizontal configuration), both experimental observation [6] and numerical modeling [7] suggest that even with a strong magnetic furnace (5-Tesla constant axial magnetic field), the convective flow in the melt still cannot be sufficiently suppressed to reach the diffusion-controlled level. In order to completely dampen the buoyancy-induced convection on earth, estimates based on scaling analysis indicate that for common experimental conditions, an extremely high magnetic field is required, far beyond the capacity of the experimental apparatus currently available. Therefore, it is proposed that only the combination of microgravity environment and magnetic damping will produce the desired diffusion-controlled growth state for this particular material.

The primary objectives of this study are to provide a quantitative understanding of the complex transport phenomena during solidification of non-dilute binarys, to furnish a numerical tool for furnace design and growth condition optimization, to provide estimates of the required magnetic field strength for low gravity growth, and to assess the role of magnetic damping for space and earth control of the double-diffusive convection. As an integral part of a NASA research program, our numerical simulation supports both the flight and ground-based experiments in an effort to bring together a complete picture of the complex physical phenomena involved in the crystal growth process.

---

[a]. NASA, Langley Research Center, Hampton, VA 23681 (retired)

[b]. NASA, Langley Research Center, Hampton, VA 23681

[c]. NRC, Langley Research Center, Present address: Northrop Grumman STC, Pittsburgh, Pa 15235

[d]. NASA, Lewis Research Center, Cleveland, OH 44135

[e]. Ohio AeroSpace Institute, Brook Park, OH 44142

[f]. NASA Marshall Space Flight Center, Huntsville, AL 35812

2. MATHEMATICAL MODEL

2.1 Magnetohydrodynamic Models

In the literature [8], there are mainly three approximations for the MHD equations. The most complex approximation incorporates the interaction between fluid flow and the magnetic field and its derivation can be found in [9]. This model is valid for describing MHD effects in electrically conducting melts of non-magnetic metals or semiconductors in which Ohm's law is valid and the fluid velocity is small compared to the speed of light.

The second is a more restrictive approximation which assumes that the fluid flow does not disturb the externally applied field with the Lorentz force still being present. This approximation is valid if the magnetic Reynolds number and the magnetic Prandtl number are both small which is the case in typical crystal growth of semiconductors. The derivation of the governing MHD equations can be found in [10].

The third and simplest MHD model is the so-called induction free approximation. In this approximation, any induced electrical field is set to be identically zero and thereby the MHD effects of the imposed field can be solely expressed through the Lorentz force term in the momentum equation. Because the magnetic Reynolds number is negligibly small under the growth conditions considered herein, this model applies well to our case and is used in the present study.

2.2 Governing Equations

In this paper, the liquid pseudo-binary mixture of LTT is assumed to behave as a Newtonian fluid and its motion is described by the Navier-Stokes equation. Other governing equations include the incompressibility condition, energy equation and concentration equation, plus the phase change conditions at the solid/liquid interface and the appropriate boundary conditions.

2.3 The FEM Model

We consider vertical and horizontal Bridgman growth configurations. For bottom seeded (vertical) Bridgman growth with axisymmetric boundary conditions, it is reasonable to assume that the heat, species and flow fields are all axisymmetric.

The so-called pseudo-steady-state model (PSSM) [11] is adopted in the present work. In PSSM, the directional steady movement of the solid/liquid interface during the steady growth is modeled by letting melt enter at its hot end with a uniform growth velocity and composition and by removing the crystal from the cold end at a speed that conserves the mass of the alloy in the system. This simplification is valid for long ampoules and melts with low Prandtl numbers, in which the transient effects on heat transfer are small [12].

The axisymmetric and 2-D FEM models are built with the 4-node bilinear element, in which velocity, temperature and species are approximated by bilinear shape functions. The pressure is

approximated as piecewise constant. The moving solid-liquid interface is modeled by the front-tracking technique [13]. To update the interface position and remesh the interior domains, a method of spines [14,15] is used. The nonlinear algebraic system resulting from the FEM discretization procedure is solved by a segregated solution approach. Details of the FEM formulation in FIDAP are documented in [14]. The nonlinear iteration termination is controlled by a specified tolerance of for the relative error norms of velocity, residual and free surface update.

3. NUMERICAL RESULTS

The action of an axial magnetic field on convection in the melt is to interfere with the radial velocity component. At large magnetic field strength, the magnitude of the radial velocity is inversely proportional to the square of the strength of magnetic field [11]. The axial velocity component is not affected by the magnetic field except in the coupling through the incompressibility condition. When the field is large enough, an almost uniaxial flow can always be obtained. One of the goals of this study is to quantitatively determine the required magnetic field levels at which the diffusion-controlled growth can be achieved in orbit. In this section we provide a typical analysis of magnetic damping for vertical Bridgman growth at a low gravity of . Our numerical results suggest that the influence of magnetic damping on the convective flow in the melt is indeed very effective. There are two large counter-rotating flow cells throughout the liquid region indicating the existence of significant convection caused by both thermal and solutal buoyancy forces. At 3kG, the convective flow is greatly affected and the flow cells become much smaller corresponding to much weaker convective strength. It is interesting to note that there is a critical value between 3.0 and 3.14kG for this specific problem. When B exceeds this critical value, the flow cells are completely suppressed. At B=9.6kG, the streamlines become perfectly straight which suggests that a diffusion-dominated growth state has been achieved.

We next examine the effects of magnetic damping on the solute segregation. Solute segregation phenomena on the macroscopic scale can be divided into two classes; namely longitudinal (axial) macro segregation caused by mixing on the melt length scale and transverse (radial) segregation caused by low levels of mixing near the interface and by interface curvature. As analyzed by D.H. Kim et al [11], these two forms of segregation are a function of convection level in the melt. In our computation, we consider variable-level magnetic damping under a constant gravity level and a fixed set of furnace parameters. Consequently the convective strength, and hence the solute segregation, is directly related to the strength of the imposed magnetic field. The solute field is visualized via iso-concentration contour plots, which illustrates qualitatively how solute segregation changes with increase of magnetic field. The axial solute segregation is greatly reduced at 3 kG and an almost diffusion-dominated growth (characterized by the thin diffusion boundary layer near the interface) is reached at 9.6 kG.
In order to quantitatively describe the effects of magnetic damping and the transition from growth with intensive laminar convective mixing to diffusion-controlled growth (without bulk convection), we compute three representative quantities. The first is the maximum total velocity, which can be used as a measure of the convective strength in the melt. Note that the total velocity includes a constant translation velocity (the growth rate) and the buoyancy-induced convective flow velocity. The results are given in Figure 1. The U_{max} v.s. B curve given in

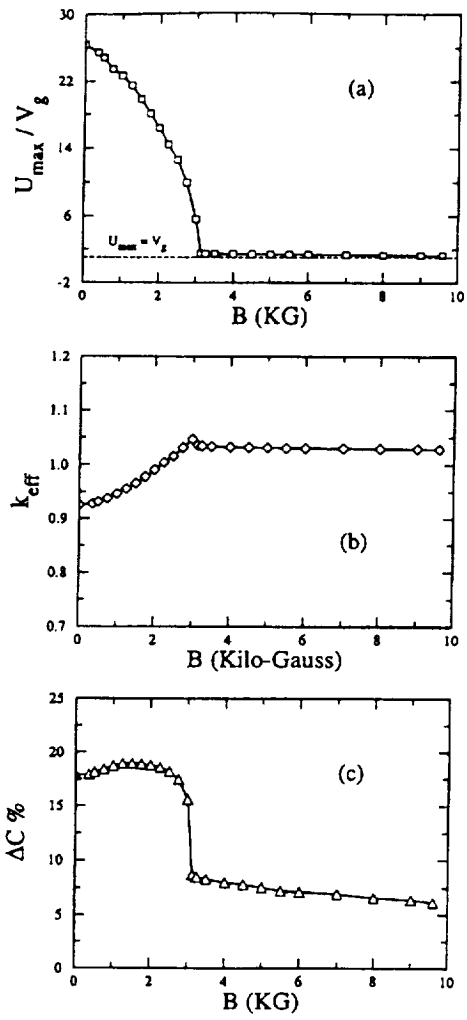

Figure 1. Quantitative descriptions of the effect of magnetic damping on convective flow strength and solute segregation in the PbSnTe melt. (a) The total maximum velocity; (b) The effective segregation coefficient, (c) The percentage radial segregation.

Figure 1(a) shows that there are two stages during the magnetic damping process. The first is a rapid change stage in which the strength of the convective flow in the melt is greatly reduced with an increase of B. The second is a slow (asymptotic) change stage during which the velocity decreases very slowly with the increase of B. These two stages are divided by the critical field value, B_c (in this particular example) and can be clearly seen in Figure 1(a). In this case, over 90% of the original strength of convection is damped when is increased from zero to about 3 kG. However it requires an additional 6 kG or more to eliminate nearly all of the original velocity strength.

The second quantified parameter is the effective segregation coefficient k_{eff}. The third is the percentage radial segregation. Radial segregation results show that both weak and strong convection levels produce low radial segregation, while intermediate convection levels produce high radial segregation [16]. The computed segregation coefficients for vertical growth are plotted as a function of levels in Figures 1(b) and (c). The two stages mentioned above can be easily distinguished. It is seen from Figure 1(b) that increases effectively in the first stage ($0<B<B_c$) and then asymptotically approaches unity at the second stage ($B>B_c$). k_{eff}~1 indicates quantitatively that the desired diffusion-controlled growth state is indeed achieved at B=9.6kG . Figure 1(c) shows how radial segregation changes with increasing B, while the expected qualitative behavior of the radial segregation is evident from Figure 1(c), it is clear that during the first stage, the reduction in flow strength only minimally affects the local segregation conditions near the interface. The almost complete stoppage of convection around has a dramatic effect on the radial segregation with a slow asymptotic regime at higher magnetic field strength.

The analysis presented in this section is limited to the vertical growth under microgravity. At high gravity levels (e.g. at full earth gravity level), our results suggest that the axially imposed magnetic field is not effective for suppressing convective flow in the PbSnTe melt. A typical example of magnetic damping for the vertical growth of PbSnTe on earth was shown in [17], which suggests that the maximum fluid velocity is still about 1000 times higher than crystal growth rate at 60 kG and the decrease of the fluid velocity is much slower than that at the microgravity gravity levels.

4. EXPERIENTIAL

The Earth based experiments are relatively straight forward. Crystals are grown in a magnetic field. After growth they are evaluated for compositional uniformity and defect structure. The experimental parameters are ampoule dimensions, temperature gradient, and magnetic field strength and orientation. The solutal driving force can be varied by both changing the growth rate, the temperature gradient, ampoule size, and by changing the starting ratio of SnTe to PbTe. Numerical analysis helps select the experimental matrix.

Experimental results to date of 1 cm diameter crystals grown in a 80 C/cm thermal gradient with growth rate as a parameter are indistinguishable from the totally mixed results obtained without magnetic fields, even with the 5T field. This result, for these conditions, was predicted by our numerical analysis.

5. CONCLUSIONS

For Bridgman growth of PbSnTe under microgravity (with both vertical and horizontal configurations), the simulations suggest that a moderate axial magnetic field of only a few kilo-Gauss in strength could effectively eliminate buoyancy-induced convection in the melt and control solute segregation. Therefore, this work confirms the idea that the combination of microgravity environment and the magnetic damping will indeed be sufficient to produce the desired diffusion-controlled growth state for PbSnTe.

REFERENCES

[1] A.L. Fripp, R.K. Crouch, W.J. Debnam, G.A. Woodell, I.O. Clark, F.M.Carlson, and R.T. Simchick: in Microgravity Science and Applications Flight Programs - Selected Papers, NASA Tech. Memorandum 4069, October 1988.

[2] M. Yao, A. Chait, A.L. Fripp and W.J. Debnam; Microgravity Sci. Tech., Vol. 8 (1996) pp. 214-225.

[3] H.P. Utech and M.C. Flemings; J. Appl.Phys., Vol. 37 (1966) pp. 2021-2024.

[4] H.P. Utech and M.C. Flemings; Crystal Growth, ed. H.S. Peiser, Pergamon Press, Oxford, 1967.

[5] H.A. Chedzey and D.T.J. Hurle, Nature, Vol. 210 (1966) p. 933.

[6] A.L. Fripp, (private communication), 1995.

[7] M. Yao, (unpublished numerical results), 1995.

[8] J. Baumgartl and G. Muller; Proc. 8th European Symposium on Materials and Fluid Science in Microgravity, Brussels, Belgium, 12-16 April, 1992, pp.161-164.

[9] P.H. Roberts; An Introduction to Magnetohydrodynamics, Longmans, London, 1967.

[10] L.D. Landau, E.M. Lifshitz and L.P. Pitaevskii; Electrodynamics of Continuous Media, Translated by J.B. Sykes, J.S. Bell, and M.J. Kearsley, 2nd ed., Pergamon Press, New York, 1984.

[11] D.H. Kim, P.M. Adornato and R. Brown; J. Crystal Growth, Vol. 89 (1988) pp. 339-356.

[12] T.J. Jasinski, W.M. Rohsenow and A.F. Witt; J. Crystal Growth, Vol. 61 (1983) p. 339.

[13] J. Crank; Free and Moving Boundary Problems, Clarendon Press, Oxford, 1984.

[14] M. Engleman; FIDAP Theoretical Manual (version 7), Fluid Dynamics International, Inc., 500 Davis St. Suite 600, Evanston, IL 60201, 1993.

[15] H. Saito and L.E. Scriven; J. Comp. Phys., Vol. 42 (1981) p. 53.

[16] M.A. Brown, AIChE J, Vol.34 (1988), pp. 881-911.

[17] M. Yao, A. Chait, A.L. Fripp and W.J. Debnam, Proceedings of the 6th FIDAP Users Conference, Chicago, IL, 4/30-5/2, 1995; also NASA Technical Memorandum 106996.